Microresonator-based comb generation without an external laser source

Adrea R. Johnson,[1] Yoshitomo Okawachi,[1] Michael R. E. Lamont,[1,2,3] Jacob S. Levy,[2] Michal Lipson,[2,3] and Alexander L. Gaeta[1,3,*]

[1]*School of Applied & Engineering Physics, Cornell University, Ithaca, NY 14853, USA*
[2]*School of Electrical and Computer Engineering, Cornell University, Ithaca, NY 14853, USA*
[3]*Kavli Institute at Cornell for Nanoscale Science, Cornell University, Ithaca, NY 14853, USA*
[*]*a.gaeta@cornell.edu*

Abstract: We demonstrate a fiber-microresonator dual-cavity architecture with which we generate 880 nm of comb bandwidth without the need for a continuous-wave pump laser. Comb generation with this pumping scheme is greatly simplified as compared to pumping with a single frequency laser, and the generated combs are inherently robust due to the intrinsic feedback mechanism. Temporal and radio frequency (RF) characterization show a regime of steady comb formation that operates with reduced RF amplitude noise. The dual-cavity design is capable of being integrated on-chip and offers the potential of a turn-key broadband multiple wavelength source.

©2014 Optical Society of America

OCIS codes: (190.4380) Nonlinear optics, four-wave mixing; (190.4390) Nonlinear optics, integrated optics.

References and links

1. T. J. Kippenberg, R. Holzwarth, and S. A. Diddams, "Microresonator-based optical frequency combs," Science **332**(6029), 555–559 (2011).
2. P. Del'Haye, A. Schliesser, O. Arcizet, T. Wilken, R. Holzwarth, and T. J. Kippenberg, "Optical frequency comb generation from a monolithic microresonator," Nature **450**(7173), 1214–1217 (2007).
3. A. A. Savchenkov, A. B. Matsko, V. S. Ilchenko, I. Solomatine, D. Seidel, and L. Maleki, "Tunable optical frequency comb with a crystalline whispering gallery mode resonator," Phys. Rev. Lett. **101**(9), 093902 (2008).
4. M. A. Foster, J. S. Levy, O. Kuzucu, K. Saha, M. Lipson, and A. L. Gaeta, "A silicon-based monolithic optical frequency comb source," arXiv:1102.0326.
5. Y. Okawachi, K. Saha, J. S. Levy, Y. H. Wen, M. Lipson, and A. L. Gaeta, "Octave-spanning frequency comb generation in a silicon nitride chip," Opt. Lett. **36**(17), 3398–3400 (2011).
6. W. Liang, A. A. Savchenkov, A. B. Matsko, V. S. Ilchenko, D. Seidel, and L. Maleki, "Generation of near-infrared frequency combs from a MgF$_2$ whispering gallery mode resonator," Opt. Lett. **36**(12), 2290–2292 (2011).
7. S. B. Papp and S. A. Diddams, "Spectral and temporal characterization of a fused-quartz-microresonator optical frequency comb," Phys. Rev. A **84**(5), 053833 (2011).
8. K. Saha, Y. Okawachi, B. Shim, J. S. Levy, R. Salem, A. R. Johnson, M. A. Foster, M. R. Lamont, M. Lipson, and A. L. Gaeta, "Modelocking and femtosecond pulse generation in chip-based frequency combs," Opt. Express **21**(1), 1335–1343 (2013).
9. F. Ferdous, H. Miao, D. E. Leaird, K. Srinivasan, J. Wang, L. Chen, L. T. Varghese, and A. M. Weiner, "Spectral line-by-line pulse shaping of an on-chip microresonator frequency comb," Nat. Photonics **5**(12), 770–776 (2011).
10. T. Herr, K. Hartinger, J. Riemensberger, C. Y. Wang, E. Gavartin, R. Holzwarth, M. L. Gorodetsky, and T. J. Kippenberg, "Universal formation dynamics and noise of Kerr-frequency combs in microresonators," Nat. Photonics **6**(7), 480–487 (2012).
11. Th. Udem, R. Holzwarth, and T. W. Hänsch, "Optical frequency metrology," Nature **416**(6877), 233–237 (2002).
12. Z. Jiang, D. E. Leaird, and A. M. Weiner, "Line-by-line pulse shaping control for optical arbitrary waveform generation," Opt. Express **13**(25), 10431–10439 (2005).
13. T. Steinmetz, T. Wilken, C. Araujo-Hauck, R. Holzwarth, T. W. Hänsch, L. Pasquini, A. Manescau, S. D'Odorico, M. T. Murphy, Th. Kentischer, W. Schmidt, and Th. Udem, "Laser frequency combs for astronomical observations," Science **321**(5894), 1335–1337 (2008).
14. T. Carmon, L. Yang, and K. J. Vahala, "Dynamical thermal behavior and thermal self-stability of microcavities," Opt. Express **12**(20), 4742–4750 (2004).
15. M. Peccianti, A. Pasquazi, Y. Park, B. E. Little, S. T. Chu, D. J. Moss, and R. Morandotti, "Demonstration of a stable ultrafast laser based on a nonlinear microcavity," Nat. Commun **3**, 765 (2012).

16. L. Caspani, M. Peccianti, A. Pasquazi, M. Clerici, L. Razzari, B. E. Little, S. T. Chu, D. J. Moss, and R. Morandotti, "Self-locked low threshold OPO in a CMOS-compatible microring resonator," CM2M.2, CLEO: Science and Innovations (2012).
17. A. Pasquazi, L. Caspani, M. Peccianti, M. Clerici, M. Ferrera, L. Razzari, D. Duchesne, B. E. Little, S. T. Chu, D. J. Moss, and R. Morandotti, "Self-locked optical parametric oscillation in a CMOS compatible microring resonator: a route to robust optical frequency comb generation on a chip," Opt. Express **21**(11), 13333–13341 (2013).
18. A. Pasquazi, M. Peccianti, B. E. Little, S. T. Chu, D. J. Moss, and R. Morandotti, "Stable, dual mode, high repetition rate mode-locked laser based on a microring resonator," Opt. Express **20**(24), 27355–27362 (2012).
19. N. A. Cholan, M. H. Al-Mansoori, A. S. M. Noor, A. Ismail, and M. A. Mahdi, "Multi-wavelength generation by self-seeded four-wave mixing," Opt. Express **21**(5), 6131–6138 (2013).
20. H. Park, A. W. Fang, O. Cohen, R. Jones, M. J. Paniccia, and J. E. Bowers, "A hybrid AlGaInAs–silicon evanescent amplifier," IEEE Photon. Technol. Lett. **19**(4), 230–232 (2007).
21. L. Agazzi, J. D. B. Bradley, M. Dijkstra, F. Ay, G. Roelkens, R. Baets, K. Wörhoff, and M. Pollnau, "Monolithic integration of erbium-doped amplifiers with silicon-on-insulator waveguides," Opt. Express **18**(26), 27703–27711 (2010).
22. P. A. M. Dirac, "The quantum theory of the emission and absorption of radiation," Proc. R. Soc. Lond., A Contain. Pap. Math. Phys. Character **114**(767), 243–265 (1927).
23. C. Y. Jin, M. Y. Swinkels, R. Johne, T. B. Hoang, L. Midolo, P. J. van Veldhoven, and A. Fiore, "All optical control of the spontaneous emission of quantum dots using coupled-cavity quantum electrodynamics," arXiv:1207.5311.
24. E. M. Purcell, "Spontaneous emission probabilities at radio frequencies," Phys. Rev. **69**, 681 (1946).
25. V. Sandoghdar, F. Treussart, J. Hare, V. Lefèvre-Seguin, J.-M. Raimond, and S. Haroche, "Very low threshold whispering-gallery-mode microsphere laser," Phys. Rev. A **54**(3), R1777–R1780 (1996).
26. D. D. Smith, H. Chang, and K. A. Fuller, "Whispering-gallery mode splitting in coupled microresonators," J. Opt. Soc. Am. B **20**(9), 1967–1974 (2003).

1. Introduction

Recent developments demonstrate that parametric four-wave mixing (FWM) in high-Q microresonators is a highly promising and effective approach for optical frequency comb generation [1–10], with applications including spectroscopy, optical clocks, arbitrary waveform generation, frequency metrology, and astronomical spectrograph calibration [1,11–13]. Frequency comb generation in each of these microresonator platforms requires tuning an external, single-frequency, continuous-wave (cw) laser into a resonance of the microresonator. As the pump power is coupled into the microresonator, thermal effects shift the resonance to higher wavelengths, creating a soft thermal lock between the cavity resonance and the pump laser [14]. When the intracavity power exceeds the threshold for parametric oscillation, cascaded four-wave mixing and higher-order four-wave mixing processes occur, resulting in comb generation. Fluctuations in the frequency or power of the pump laser can detune the pump out of the cavity resonance, which disrupts comb generation. These limitations can be overcome using a drop-port of the microresonator as shown by Peccianti *et al.* [15–18] with a hydex microring imbedded in a fiber cavity pumped with an erbium-doped fiber amplifier (EDFA). Through filter-driven four-wave mixing, they demonstrate a high-repetition-rate pulse source with a 60-nm bandwidth and a 200-GHz repetition rate. In this drop-port configuration the microresonator acts as a filter, seeding the EDFA with wavelengths that correspond to resonances of the microresonator, similar to the recent work done by Cholan, *et al.* [19] for realization of a multiple wavelength source.

Here, we explore a dual-cavity architecture where a single bus waveguide (through-port), which forms part of the external fiber cavity, is coupled to the microresonator (Fig. 1). Due to the higher density of photonic states in the microresonator as compared to the fiber cavity, preferential emission occurs at the microresonator modes resulting in lasing and parametric comb generation defined by the microresonator. Our through-port configuration is effectively analogous to microresonator-based comb generation using a cw pump laser. Additionally, since only a single bus waveguide is coupled to the microresonator, the system operates with reduced coupling losses and allows for higher power efficiency.

Through the use of this dual-cavity design, we achieve broadband comb generation spanning more than 880 nm. Key advantages of this scheme are that the system requires only a narrow-band optical amplifier, as opposed to a stabilized single-frequency laser, and that it eliminates the need to pump at and tune to a resonance wavelength which eliminates

disruptions to comb generation due to pump frequency fluctuations which can shift the pump out of resonance. Such a scheme could greatly simplify the comb generation process and allow for a fully-integrated chip-scale multiple-wavelength source with an on-chip amplifier [20,21].
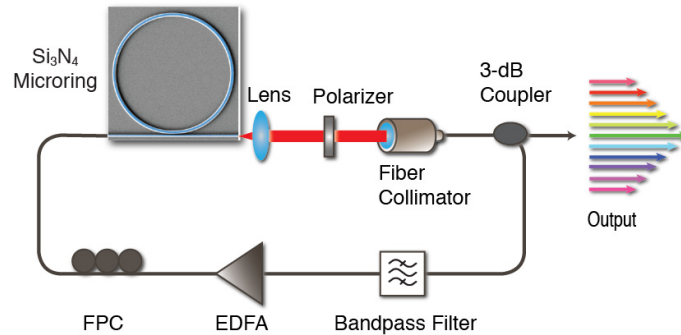
2. Experiment

Fig. 1. Experimental setup for comb generation. The system is based on a dual-cavity design consisting of the silicon-nitride microresonator and an external fiber cavity.

Our dual-cavity-based scheme for comb generation is shown in Fig. 1. Amplified spontaneous emission (ASE) from an EDFA is coupled into a silicon-nitride microresonator. A fiber polarization controller (FPC) allows for adjustment of the polarization of light coupled to the microresonator, which is a critical issue for cw lasing of the external fiber cavity and comb generation. A polarizer is placed at the output to select quasi-TE polarization. The dispersion of the microresonator waveguide is engineered to optimize parametric FWM gain and oscillation for the TE modes. After the microresonator, a 3-dB coupler is used for output coupling, and the remaining light in the external cavity is passed through a fixed bandpass filter and fed back into the EDFA. The bandpass filter allows for control of the spectral region that experiences round-trip EDFA gain.

Our system achieves comb generation through a different mechanism as compared to the filter-driven FWM process utilizing the drop-port of the microresonator [15–18]. In the drop-port configuration, the microresonator effectively acts as both the nonlinear element and as a filter which selects the wavelengths that correspond to resonances of the microresonator for amplification in the EDFA. In our system, depending upon the state of the input polarization, lasing of the dual-cavity can be achieved at modes corresponding to the external fiber cavity or at modes of the microresonator. Initially, it may be counterintuitive that the cavity lases at microresonator resonances at which the round-trip cavity losses are higher. However, the mechanism can be understood in terms of the transition probability as dictated by Fermi's Golden Rule [22,23]. Below the lasing threshold, the probability of the system emitting at either a microresonator mode or a mode of the external fiber cavity is directly proportional to the density of available states at that frequency. The enhancement of the density of states in a cavity is given by the Purcell factor $F_p = (3\lambda^3/4\pi^2)(Q/V)$ where Q is the quality factor and V is the mode volume [24]. While the loaded Q-factor of the microresonator, when considering the cold-cavity modes, is lower than that of the external cavity by approximately a factor of 100, the mode volume of the microresonator cavity is lower by a factor of 10^6, in which case the microresonator resonances provide a higher density of states and thus a higher transition probability to the frequencies corresponding to the microresonator resonance. Since the threshold power for lasing contains the same V/Q factor [25], the modes corresponding to the microresonator cavity reach the oscillation threshold before the external fiber cavity. With sufficient power buildup, the microresonator cavity reaches oscillation threshold, at which point, frequency dependent EDFA gain will preferentially amplify the oscillating mode(s) to the point where it can serve as a pump for comb generation. For comb generation, the

polarization is adjusted to quasi-TE, as the coupling between the microresonator and the bus waveguide is optimized for the TE mode. When the polarization is adjusted away from quasi-TE, the Q-factor of the microresonator cavity decreases relative to that of the fiber cavity, and lasing occurs in modes corresponding to the external fiber cavity.

To further understand this behavior, we simulate the lasing behavior in our system based on the coupled ring resonator model [26]. Figure 2 shows the dynamics of the output of the dual-cavity system as the system reaches steady state. Figure 2(a) shows the system initially pumped with ASE. Initially, as the power builds up, the spectrum shows dips corresponding to resonances of the microresonator [Fig. 2(b)]. Due to its higher Purcell factor from the high modal confinement, the microresonator intracavity power continues to build with each successive round trip and reaches threshold for lasing before the external cavity. The lasing mode in the microresonator builds up further and dominates the external cavity modes resulting in the overall dual-cavity system lasing at modes corresponding to the microresonator [Figs. 2(c)-2(e)]. If the cavity loss of the microresonator is increased leading to a corresponding decrease in the cavity Q-factor, the dual-cavity system can be shown to lase at modes of the external fiber cavity away from the microresonator resonances.
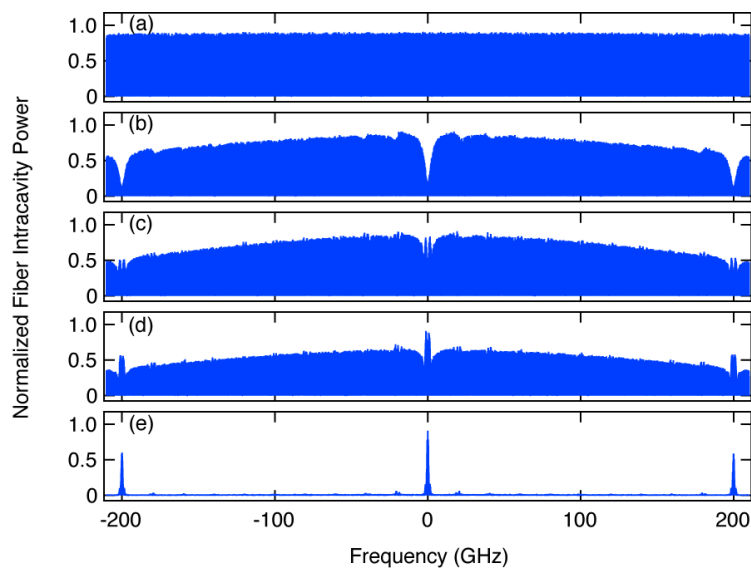

Fig. 2. Spectra illustrating the dynamics of the dual-cavity intracavity power in the fiber cavity as the system reaches steady state. (a) Initial state is seeded with noise. (b) Power in the fiber modes exceeds the power in the microresonator modes. (c)-(d) Buildup of intracavity power in the microresonator. (e) Lasing of the system at modes of the microresonator.

We experimentally investigate the lasing behavior at the modes of the microresonator and external fiber cavities using the dual-cavity setup minus the bandpass filter. We pump at low EDFA power such that the system is near the lasing threshold and adjust the polarization to select the lasing wavelength of the system. For quasi-TE polarization, Fig. 3(a) illustrates lasing at modes of the microresonator for a range of power levels coupled into the bus waveguide. Dips in the optical spectrum correspond to TM resonances of the microresonator. Adjusting the polarization away from quasi-TE leads to lasing at modes of the external cavity away from the microresonator resonances [see Fig. 3(b)]. The modulations in the spectra result from the Fabry-Perot effect caused by reflections from the facets of the bus waveguide. Slight dips in the spectrum at 1542.5 nm and 1544.3 nm correspond to losses due to the TE resonances of the microresonator. The lasing wavelength of the dual-cavity system can therefore be selected through the state of the input polarization.
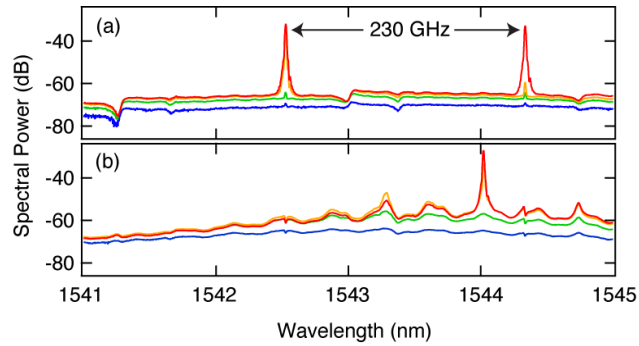
Fig. 3. Output spectra of the dual-cavity system for a range of power levels in the bus waveguide. (a) Dual-cavity system oscillating at modes of microresonator. (b) Dual-cavity system oscillating at an external fiber cavity mode away from microresonator resonances.

The dependence of the dual-cavity lasing wavelength on the state of the input polarization to the microresonator is further illustrated in Fig. 4 which shows how the dual-cavity lasing mode shifts to modes of the microresonator as the polarization is adjusted toward quasi-TE. The system starts away from the quasi-TE polarization state, resulting in lasing at modes of the external fiber cavity away from the microresonator modes (top). Adjustment of the polarization towards TE can lead to an intermediate state where the system is lasing at both an external cavity and microresonator mode. Further optimization of the polarization results in lasing at a microresonator mode. And finally, for quasi-TE polarization, the system achieves lasing at modes of the microresonator and the generation of a frequency comb (bottom).
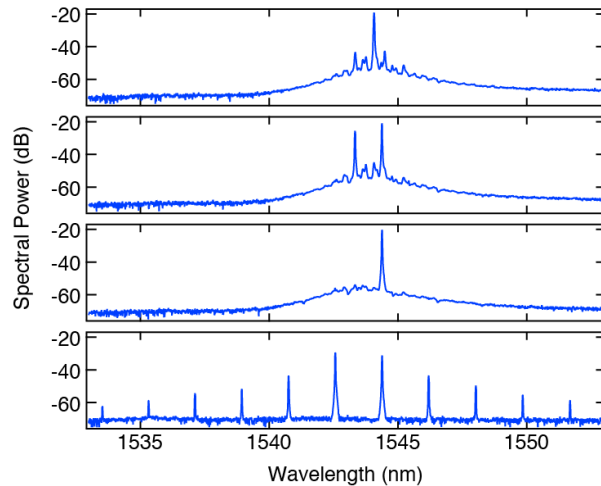

Fig. 4. Measured optical spectra as the polarization is adjusted towards quasi-TE (bottom). The system makes transitions from lasing in an external fiber cavity mode, away from a microresonator mode, to lasing and comb generation in a microresonator mode.

We apply the dual-cavity design to produce a broad comb spectra using a 230-GHz free spectral range (FSR) microresonator with a waveguide cross section of 725 x 1600 nm to provide a broad region of anomalous dispersion which yields a comb spectrum spanning 880 nm (90 THz) with over 390 comb lines when pumped with 2.17 W of EDFA power [Fig. 5(a)]. For a microresonator with an 80-GHz FSR and 725 x 1700 nm cross section a bandwidth of 730 nm (78 THz) [Fig. 5(b)] is achieved with 2 W of EDFA power.
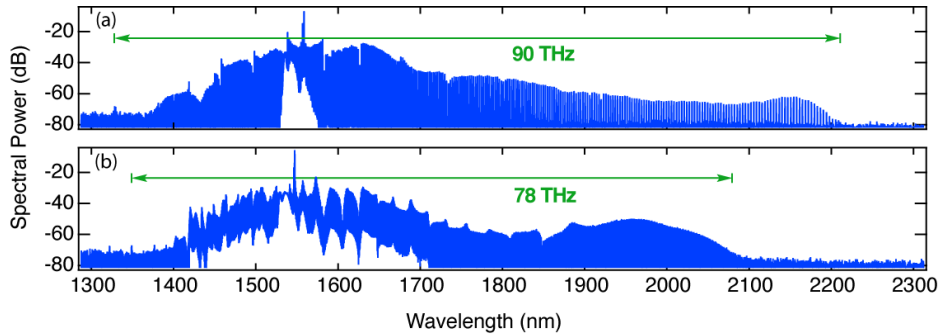
Fig. 5. Parametric frequency comb spectra generated from silicon-nitride microresonators with FSR's of (a) 230-GHz and (b) 80-GHz.

We confirm that comb generation in this system is similar to that using an external cw pump laser by utilizing a 1.1-nm bandpass filter whose bandwidth is narrower than the FSR of the microresonator. This restricts the amplifier bandwidth to a narrow region surrounding a single microresonator resonance. Figure 6 shows broadband comb generation for the bandpass filter centered at 1544 and 1558.7 nm. In both cases the single lasing peak is responsible for the generation of the comb.
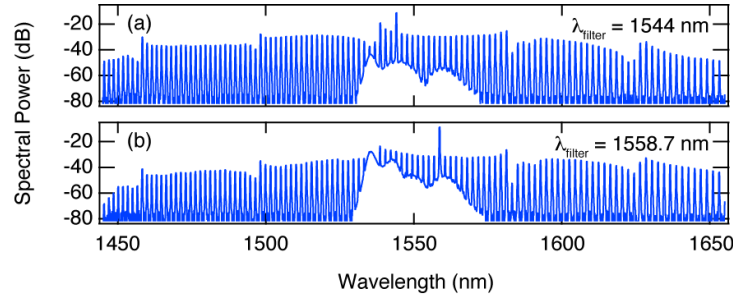
Fig. 6. Dual-cavity-based comb generation with a 1.1 nm bandpass filter centered at (a) 1544 nm and, (b) 1558.7 nm.

We next characterize the dual-cavity based frequency comb spectrum in the time domain by sending the entire output to a fast photodiode and measuring the signal using a 6-GHz real-time oscilloscope. The state of the frequency comb depends significantly on the polarization of light injected into the microresonator. By adjusting the polarization, we are able to produce two distinct comb states, shown in Fig. 7. Figure 7(a) displays the frequency comb spectrum corresponding to the single-shot temporal measurement shown in Fig. 7(c). The slow temporal modulations, which occur every 18 μs, are due to Q-switching within the external cavity due to gain saturation of the EDFA [18]. With small adjustments to the input polarization, we are able to achieve a steady state for comb generation absent of Q-switching. Figure 7(b) shows the comb spectrum and Fig. 7(d) shows the temporal measurement corresponding to this non-Q-switching state. Similar transition behavior from Q-switching has been observed by Pasquazi, *et al* [18].
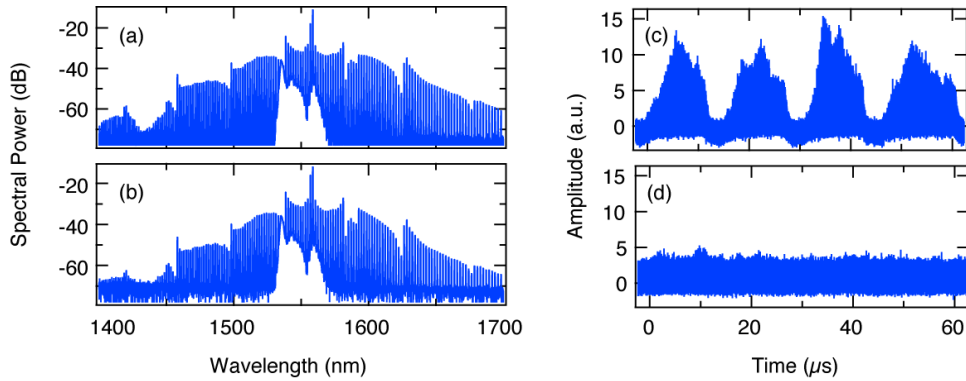
Fig. 7. (a) Optical frequency comb spectra for the system in the Q-switched state and (b) the corresponding real-time temporal measurement. (c) Comb spectrum for non-Q-switched case and (d) the corresponding temporal measurement.
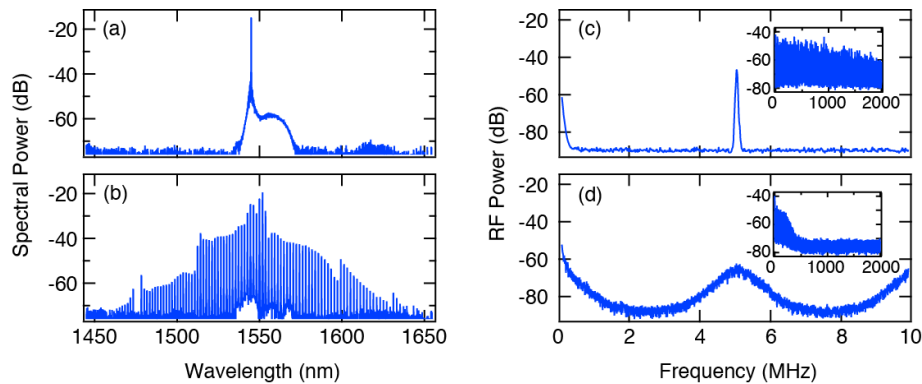

Fig. 8. Optical output spectra without (a) and with (b) coupling to the microresonator and (c) and (d) are the corresponding RF spectra, respectively. The insets in (c) and (d) show the RF noise from DC to 2 GHz.

In order to understand the spectral properties of our dual-comb system, we perform simultaneous RF and optical spectral measurements of the dual-cavity output. We utilize the dual-cavity configuration with the bandpass filter removed from the external fiber cavity. By adjusting the polarization, we allow the external fiber cavity to lase without interaction with the resonator [see Fig. 8(a)]. The output from the bus waveguide is detected with a 12.5-GHz photodiode, and the resulting RF signal is amplified with a 0.1-500-MHz low-noise amplifier and measured using an RF spectrum analyzer. The detected RF beatnote is 5 MHz [Fig. 8(c)], which corresponds to beating of the external cavity modes since the 1-GHz linewidth of the microresonator mode supports multiple modes of the external cavity. The inset in Fig. 8(c) further illustrates this multi-mode behavior as the RF noise is present out to 2 GHz. Next, the polarization in the bus waveguide is rotated to quasi-TE for comb generation and the entire comb output is sent to the photodiode and RF amplifier for characterization. The measured optical power at the photodiode is equal to that for the case of lasing in the fiber cavity. When a state of steady comb generation is reached [Fig. 8(b)], despite the multi-mode pump, a steady state of comb generation can be reached in which the RF amplitude of the 5 MHz beatnote is reduced by 20 dB, and the beatnote linewidth broadens significantly [Fig. 8(d)]. In addition, Fig. 8(d) inset shows 220 MHz (3-dB bandwidth) of RF noise during comb generation, indicating that the number of oscillating external cavity modes is greatly reduced when comb generation occurs. We believe the system can be further improved to allow for single-mode operation by reducing the external cavity length. Additionally, we expect that complete stabilization of the comb can be achieved through FSR control of both the

microresonator and external fiber cavity. Microresonator FSR stabilization can be implemented through pump power or temperature control, while stabilization of the external fiber cavity FSR can be performed using a piezo-based delay arm.

Finally, we perform measurements to determine the parametric oscillation threshold of the dual-cavity system. Figure 9 shows the optical spectra obtained for a range of EDFA pump powers. Taking into account a 6-dB coupling loss per facet, we obtain a frequency comb with 30 nm of bandwidth with 26 mW in the bus waveguide (top). Decreasing the EDFA pump power decreases the comb bandwidth until the threshold for parametric oscillation is reached (third row). Parametric oscillation occurs for an EDFA pump power of 20 mW, corresponding to 5 mW in the bus waveguide. The low oscillation threshold of the dual-cavity system and the robust nature of the comb generation suggest a promising platform that can be integrated to create a compact, turn-key multiple wavelength source.
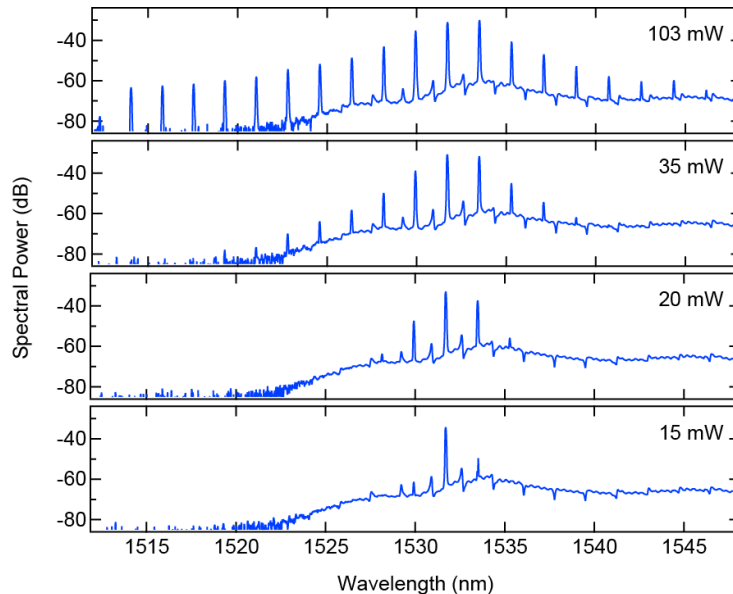

Fig. 9. Optical spectra for EDFA pump powers ranging from 15 to 103 mW. Parametric oscillation is obtained for an EDFA pump power of 20 mW (third row).

Conclusion

In conclusion, we have demonstrated a dual-cavity design to produce broadband parametric frequency comb generation spanning 90 THz without the need of an external pump laser. As a result of the higher photonic density of states of the microresonator as compared to that of the fiber cavity, the system lases at a microresonator resonance which eliminates the need to carefully tune a cw laser into a cavity resonance and results in comb generation that is inherently robust. Future designs could allow for the inclusion of an on-chip amplifier into the dual-cavity design to realize a fully-integrated, chip-scale, ultra-broadband multiple wavelength source.

Acknowledgments